AMERICAN SOCIETY FOR MICROBIOLOGY | Journal of Bacteriology

L-Hydroxyproline and D-Proline Catabolism in *Sinorhizobium meliloti*

Siyun Chen,[a] Catharine E. White,[a] George C. diCenzo,[a] Ye Zhang,[a] Peter J. Stogios,[b] Alexei Savchenko,[b] Turlough M. Finan[a]

Department of Biology, McMaster University, Hamilton, Ontario, Canada[a]; Department of Chemical Engineering and Applied Chemistry, University of Toronto, Toronto, Ontario, Canada[b]

ABSTRACT

Sinorhizobium meliloti **forms N_2-fixing root nodules on alfalfa, and as a free-living bacterium, it can grow on a very broad range of substrates, including L-proline and several related compounds, such as proline betaine, *trans*-4-hydroxy-L-proline (*trans*-4-L-Hyp), and *cis*-4-hydroxy-D-proline (*cis*-4-D-Hyp). Fourteen *hyp* genes are induced upon growth of *S. meliloti* on *trans*-4-L-Hyp, and of those, *hypMNPQ* encodes an ABC-type *trans*-4-L-Hyp transporter and *hypRE* encodes an epimerase that converts *trans*-4-L-Hyp to *cis*-4-D-Hyp in the bacterial cytoplasm. Here, we present evidence that the HypO, HypD, and HypH proteins catalyze the remaining steps in which *cis*-4-D-Hyp is converted to α-ketoglutarate. The HypO protein functions as a D-amino acid dehydrogenase, converting *cis*-4-D-Hyp to Δ^1-pyrroline-4-hydroxy-2-carboxylate, which is deaminated by HypD to α-ketoglutarate semialdehyde and then converted to α-ketoglutarate by HypH. The crystal structure of HypD revealed it to be a member of the *N*-acetylneuraminate lyase subfamily of the $(\alpha/\beta)_8$ protein family and is consistent with the known enzymatic mechanism for other members of the group. It was also shown that *S. meliloti* can catabolize D-proline as both a carbon and a nitrogen source, that D-proline can complement L-proline auxotrophy, and that the catabolism of D-proline is dependent on the *hyp* cluster. Transport of D-proline involves the HypMNPQ transporter, following which D-proline is converted to Δ^1-pyrroline-2-carboxylate (P2C) largely via HypO. The P2C is converted to L-proline through the NADPH-dependent reduction of P2C by the previously uncharacterized HypS protein. Thus, overall, we have now completed detailed genetic and/or biochemical characterization of 9 of the 14 *hyp* genes.**

IMPORTANCE

Hydroxyproline is abundant in proteins in animal and plant tissues and serves as a carbon and a nitrogen source for bacteria in diverse environments, including the rhizosphere, compost, and the mammalian gut. While the main biochemical features of bacterial hydroxyproline catabolism were elucidated in the 1960s, the genetic and molecular details have only recently been determined. Elucidating the genetics of hydroxyproline catabolism will aid in the annotation of these genes in other genomes and metagenomic libraries. This will facilitate an improved understanding of the importance of this pathway and may assist in determining the prevalence of hydroxyproline in a particular environment.

4-Hydroxyproline and 3-hydroxyproline in animal and plant proteins are formed through the posttranslational modification of proline residues by the enzyme proline hydroxylase. In some bacteria, hydroxyproline is synthesized from free L-proline, where it is employed in the synthesis of secondary metabolites (1, 2). 4-Hydroxyproline has two chiral carbon atoms, and of its four isomeric forms, *trans*-4-hydroxy-L-proline (*trans*-4-L-Hyp) and *cis*-4-hydroxy-D-proline (*cis*-4-D-Hyp) appear to be the two most common isomers. *trans*-4-L-Hyp is one of the most abundant amino acids in animals, where it is a major constituent of collagen (3). In plants and algae, several abundant cell wall proteins and glycoproteins are rich in hydroxyproline (4, 5). Other proline derivatives, such as hydroxyproline betaine and proline betaine (*N*,*N*-dimethylproline, stachydrine), are present in alfalfa and some other plants, and these are generally associated with osmotic adaptation (6–8).

Hydroxyprolines represent rich sources of nitrogen and carbon for microorganisms in soil and other environments containing decomposing biological material (9, 10). Microorganisms that utilize hydroxyproline for growth have been isolated from soil, and a pathway for the catabolism of *trans*-4-L-Hyp by *Pseudomonas* was elucidated by Adams and coworkers in the 1960s (see reference 11 and references therein). In this pathway, *trans*-4-L-Hyp is epimerized to *cis*-4-D-Hyp by hydroxyproline 2-epimerase. The *cis*-4-D-Hyp is then oxidized to Δ^1-pyrroline-4-hydroxy-2-carboxylate (HPC) by a D-hydroxyproline dehydrogenase enzyme containing flavin cofactors (12). This enzyme was previously referred to as *cis*-4-D-Hyp oxidase (11) (Fig. 1). HPC is subsequently deaminated to α-ketoglutarate semialdehyde (α-KGSA) by Δ^1-pyrroline-4-hydroxy-2-carboxylate deaminase, and in the final step, α-KGSA is oxidized by α-KGSA dehydrogenase to the central tricarboxylic acid cycle intermediate α-ketoglutarate (α-KG). Until recently, there have been few molecular analyses of the underlying genes and enzymes involved in the hydroxyproline catabolic pathway (12–14). Hence, the genes coding for hydroxyproline transport and metabolism are poorly annotated in bacterial

Received 3 December 2015 **Accepted** 25 January 2016

Accepted manuscript posted online 1 February 2016

Citation Chen S, White CE, diCenzo GC, Zhang Y, Stogios PJ, Savchenko A, Finan TM. 2016. L-Hydroxyproline and D-proline catabolism in *Sinorhizobium meliloti*. J Bacteriol 198:1171–1181. doi:10.1128/JB.00961-15.

Editor: P. J. Christie

Address correspondence to Turlough M. Finan, finan@mcmaster.ca.

S.C. and C.E.W. contributed equally to this article.

Supplemental material for this article may be found at http://dx.doi.org/10.1128/JB.00961-15.

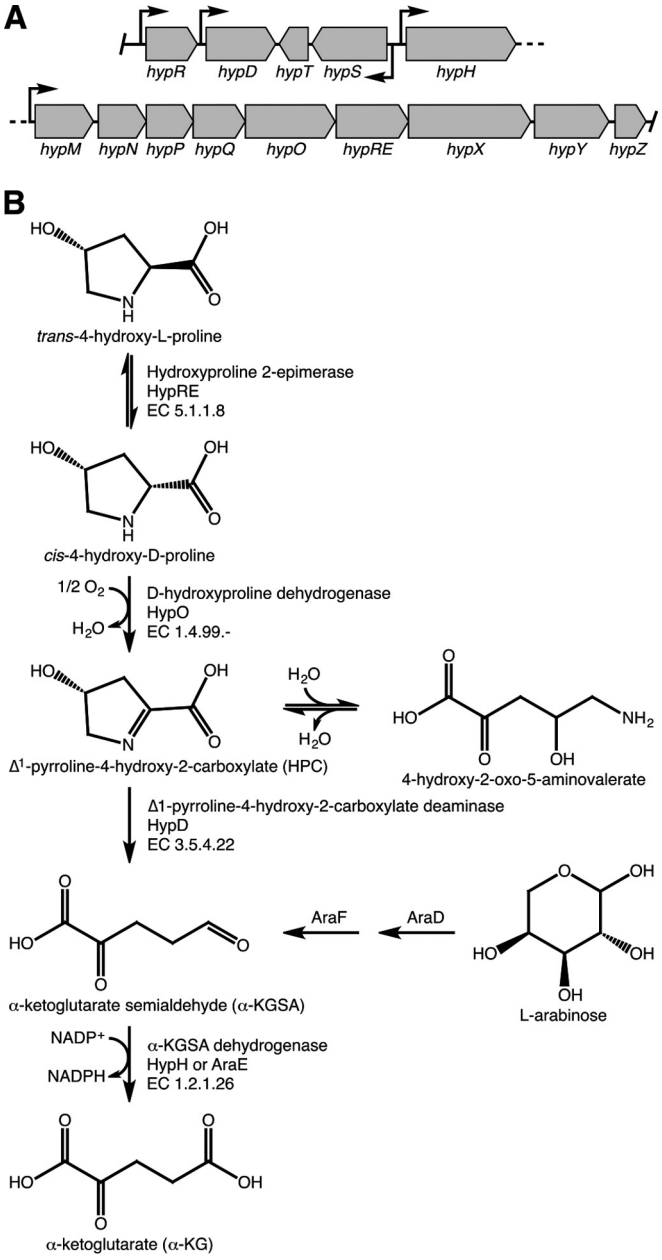

FIG 1 Genetics and biochemistry of hydroxyproline metabolism in *S. meliloti*. (A) Diagram of the hydroxyproline transport and catabolic locus; (B) schematic diagram of the hydroxyproline catabolic pathway, as described by Adams and Frank (11). (A and B) Gene annotations, promoters, and enzymatic functions as deduced through this study and previous work (13, 14, 18). HypR, negative regulator; HypD, Δ^1-pyrroline-4-hydroxy-2-carboxylate deaminase; HypT, unknown; HypS, Δ^1-pyrroline-2-carboxylate reductase; HypH, α-ketoglutarate semialdehyde dehydrogenase; HypMNPQ, L-hydroxyproline ABC-type transport system; HypO, *cis*-4-hydroxy-D-proline dehydrogenase; HypRE, hydroxyproline 2-epimerase; HypX, unknown; HypY, unknown, a possible proline racemase pseudogene; HypZ, unknown.

genomes. The abundance of genome, metagenome, and transcriptome sequences is increasing the utility and insights from having well-defined gene-function relationships for catabolic pathways. Thus, elucidating the gene-function relationships for metabolic pathways is of broad importance.

Sinorhizobium meliloti grows as a free-living bacterium in soil, and it also forms N_2-fixing root nodules on alfalfa. This bacterium grows rapidly on 4-hydroxyproline as a sole carbon and nitrogen source, and in earlier work, we identified a cluster of 14 *hyp* genes, located on the *S. meliloti* pSymB chromid, whose expression is induced by *trans*-4-L-Hyp (13, 14). The *trans*-4-L-Hyp catabolic pathway in *S. meliloti* appears to be the same as that originally characterized in *Pseudomonas* (11). In *S. meliloti*, the *hyp* gene cluster includes five operons (Fig. 1), and transcription of each is repressed by the negative regulator, HypR. Repression is relieved by *trans*-4-L-Hyp and more strongly by *cis*-4-D-Hyp, the first catabolite (14). Uptake of *trans*-4-L-Hyp and *cis*-4-D-proline is mediated by the HypMNPQ ABC-type transport system (13), and the first step in the catabolic pathway (epimerization) is performed by the *hypRE* gene product (14). The *hypO*, *hypD*, and *hypH* genes were predicted to encode *cis*-4-D-Hyp dehydrogenase, (HPC) deaminase, and α-KGSA dehydrogenase, respectively, but were not biochemically illustrated (14).

Watanabe and coworkers recently identified and characterized the D-hydroxyproline dehydrogenase and HPC deaminase enzymes from *Pseudomonas putida* and *Pseudomonas aeruginosa* (12). The D-hydroxyproline dehydrogenase enzymes from these organisms appear to have arisen via convergent evolution, where the *P. aeruginosa* enzyme contained three different subunits while the *P. putida* enzyme was a single-subunit protein (12).

In the present report, we present genetic and biochemical data that confirm the assignments of the HypD and HypH proteins and the involvement of the HypO protein in hydroxyproline catabolism. We present the high-resolution structure of HypD, which shows strong similarity to members of the *N*-acetylneuraminate lyase (NAL) enzyme subfamily of $(\alpha/\beta)_8$ barrel proteins, most significantly at the active site (12, 15). We also show that *S. meliloti* can catabolize D-proline as a carbon and nitrogen substrate and that the *hyp* gene cluster is involved in the catabolic pathway. We characterize the *hypS* gene and show that it encodes a pyrroline-2-carboxylate reductase that reduces pyrroline-2-carboxylate to L-proline. This activity is required for the growth of *S. meliloti* on D-proline but not on *trans*-4-L-Hyp or *cis*-4-D-Hyp.

MATERIALS AND METHODS

Bacterial strains, plasmids, and mutant construction. All *S. meliloti* strains are derived from RmP110, which is Rm1021 carrying a wild-type *pstC* gene (16). The nonpolar deletions of the *hypD*, *hypS*, *hypO*, and *hypH* genes were constructed by replacing the coding regions with the FLP recombination target (FRT)-Kan^r-FRT cassette using λ Red recombinase (17) as described for the Δ*hypRE* mutant (14). In all cases, the target gene together with approximately 300 bp of flanking DNA was PCR amplified and cloned into the Gm^r suicide plasmid, pUCP30T. The gene cloned in pUCP30T was replaced by a 1.4-kb FRT-Kan^r-FRT PCR product using pKD13 as the template and oligonucleotides whose 5′ ends were 50-bp sequences immediately 5′ and 3′ to the gene to be deleted. The resulting plasmid was then integrated into the genome of RmP110 to generate Nm^r Gm^s double-crossover recombinants in which the target gene was replaced by the FRT-Kan^r-FRT cassette. The *kan* gene was then removed using Flp recombinase (supplied on vector pTH2505) to generate nonpolar deletion mutants of RmP110 (14). Plasmid pTH2505 is unstable in *S. meliloti* and was easily cured. The final constructs were checked by PCR and sequencing across the FRT junctions. The mutant strains were RmP2506 Δ*hypO* (Δ*smb20267*), RmP2510 Δ*hypD* (Δ*smb20259*), RmP2514 Δ*hypS* (Δ*smb20261*), and RmP2516 Δ*hypH* (Δ*smb20262*). The *araE* Δ*hypH* double mutant (RmP3174) was made by transducing an *araE*::Tn*5*-B20 mutation (18) into RmP2516. To construct the Δ*hypS*

hypS$^+$ merodiploid strain RmP3272, plasmid pTH2685, containing *hypS* (*smb20261*) plus 300 nucleotides (nt) upstream and downstream in pUCP30T, was transferred into RmP2514, and Gm^r single-crossover recombinants were selected. The proline auxotroph RmP3155 was constructed by transducing ΔB161 (an ~53-kb deletion of the pSymB plasmid that removes the *smb20003* gene; Nm^r Gm^r) into a *proC*::Tn*5*-B20 strain (19, 20). The *putA* mutant SmFL5502 was identified in our previously constructed pTH1522 reporter gene fusion library of RmP110 (21). Reporter gene fusion strains and β-glucuronidase (GusA) activity were measured, as previously described (13, 14).

Growth studies. To test for the ability of *S. meliloti* strains to utilize and grow with various compounds as sole carbon sources, strains were grown in M9 mineral salts medium containing 48 mM Na_2HPO_4, 22 mM NaH_2PO_4, 8.6 mM NaCl, 18.6 mM NH_4Cl, 1 mM $MgSO_4$, 0.25 mM $CaCl_2$, 0.005 μg/ml biotin, 10 ng/ml $CoCl_2$, and a carbon source at 10 or 15 mM. When we tested for growth on nitrogen sources, NH_4Cl was omitted from the M9 growth medium. For growth curves, inoculum cultures grown overnight in LBmc (19) were washed with 0.85% NaCl and inoculated into each test medium to an optical density at 600 nm (OD_{600}) of 0.05. The growth profiles of 0.15-ml cultures were measured for 48 h with shaking in 96-well microtiter plates at 30°C, and the data were analyzed as previously described (22). The OD_{600} values presented are not corrected for path length, and unless stated otherwise, generation times were calculated between uncorrected OD_{600} values of 0.1 and 0.3.

Overexpression and purification of recombinant proteins HypD, HypH, and HypS. For overexpression of Hyp proteins with an N-terminal His_6 tag in *Escherichia coli*, the *hyp* genes were each cloned into pET28a and introduced into *E. coli* strain BL21/DE3. For overexpression, each strain was cultured at 30°C with aeration to the mid-log phase in LB medium with 25 μg/ml kanamycin. Expression of the recombinant protein was then induced by the addition of isopropyl-β-D-thiogalactopyranoside (IPTG) to 0.5 mM, and the cultures were incubated for an additional 4 h. The cultures were then cooled on ice, and the cells were harvested and resuspended in buffer containing 50 mM Tris-HCl (pH 8.0), 150 mM NaCl, and 7.5% glycerol. The cells were disrupted by a French press, and the lysates were cleared by centrifugation at 24,000 × *g* for 45 min.

Each of the recombinant proteins was purified to 95% purity with BD Talon cobalt resin, using batch elution as described in the manufacturer's instructions. The purified protein was stored at −80°C in buffer containing 20 mM HEPES (pH 7.5), 150 mM KCl, 1 mM dithiothreitol (DTT), 1 mM EDTA, and 10% glycerol. The protein concentrations were determined using Bio-Rad protein assay reagent (Bio-Rad) and bovine serum albumin as a standard.

HPC synthesis and HPC deaminase assays. As Δ^1-pyrroline-4-hydroxy-2-carboxylate (HPC) is an unstable compound that is not commercially available, all of the HPC substrate used in reactions was enzymatically synthesized and used immediately upon preparation (23, 24). HPC was synthesized from *cis*-4-D-Hyp in reaction mixtures that contained *cis*-4-D-Hyp and membrane preparations containing either *S. meliloti* HypO or purified *cis*-4-D-Hyp dehydrogenase from *P. aeruginosa* or *P. putida* as described by Watanabe et al. (12).

The purified *S. meliloti* HypD protein carrying an N-terminal His_6 tag was assayed for HPC deaminase activity by coupling its reaction to an α-ketoglutarate semialdehyde dehydrogenase (α-KGSADH) and monitoring the increased absorbance at 340 nm. The α-KGSADH enzyme used in these reactions was either purified HypH from *S. meliloti* or purified α-KGSADH protein from *Acinetobacter baylyi* (25). Similar deaminase activities were detected using either enzyme. The deaminase activity was also monitored by coupling the reaction to a purified glutamate dehydrogenase enzyme (α-KG + NH_3 + NADH + H^+ ⇔ glutamate + NAD^+) and detecting the production of ammonia. However, the detection of NH_3 formation was much less sensitive than the detection of deaminase activity using the α-KGSADH assay.

P2C synthesis and P2C reductase assays. The Δ^1-pyrroline-2-carboxylate (P2C) used in the P2C reductase reactions was synthesized from D-proline with the enzyme D-amino acid oxidase as described by Visser et al. (26). The reaction mixture consisted of 10 mmol D-proline, 0.25 mg porcine D-amino acid oxidase (Sigma-Aldrich), and 1,000 to 2,500 units bovine catalase (Sigma-Aldrich) in 25 mM ammonium bicarbonate buffer (pH 8.3), and the reaction was allowed to proceed overnight at 37°C. Electrospray mass spectroscopic (MS) analysis of the reaction mixtures before and after incubation showed the complete conversion of the D-proline to Δ^1-pyrroline-2-carboxylate (data not shown).

The HypS P2C reductase activity (27) was quantified at room temperature by measuring the decrease in absorbance at 340 nm in a 1-ml reaction mixture containing 13 μg HypS, 0.5 mM NADPH, and various concentrations of P2C in a 25 mM ammonium bicarbonate buffer (pH 8.3). The reverse reaction was quantified by measuring the increase in absorbance at 340 nm in a 1-ml reaction consisting of 100 mM Tris-HCl (pH 10.0), 13 μg HypS, 1 mM $NADP^+$, and various concentrations of L-proline.

α-Ketoglutarate semialdehyde dehydrogenase enzyme kinetics. α-KGSADH activity was quantified at room temperature by measuring the increase in absorbance at 340 nm in 1-ml reaction mixtures containing 50 mM HEPES buffer (pH 7.5), 100 mM NaCl, 0.5 mM $MgCl_2$, 2 to 3 μg HypH enzyme, α-KGSA, and $NAD(P)^+$. The K_m value for α-KGSA was determined using various concentrations of α-KGSA (4.45, 11.1, 17.8, 22.3, 35.6, 44.5, 89.0, 133.6, and 178.1 μM) and a constant concentration of 0.5 mM $NADP^+$. Kinetic measurements for $NAD(P)^+$ coenzyme were performed with 178 μM α-KGSA and various concentrations of $NADP^+$ (10, 25, 50, 100, 300, and 500 μM) or NAD^+ (0.2, 0.5, 1.0, 2.5, 4.0, 5.0, and 8.0 mM). α-Ketoglutarate semialdehyde was synthesized from D-glucarate using the *A. baylyi* enzymes D-glucarate dehydratase (ACIAD0128) and D-5-keto-4-deoxyglucarate dehydratase (ACIAD0130), which were overexpressed from *E. coli* as described in the work of Aghaie et al. (25).

Crystallization and structure determination of HypD. Purified HypD protein carrying an N-terminal His tag was crystallized at room temperature using the hanging-drop method, with 0.5 μl of 19.5 mg/ml protein solution (including 20% [wt/vol] glycerol) mixed with 0.5 μl of reservoir solution (0.2 M potassium-sodium tartrate, 20% [wt/vol] polyethylene glycol 3350 [PEG 3350]). The crystal was cryoprotected with Paratone oil. Diffraction data at 100 K were collected at the Structural Genomics Consortium (Toronto, ON, Canada) on a Rigaku FR-E SuperBright rotating copper anode source with a Rigaku R-Axis HTC detector. X-ray diffraction data were reduced with HKL-3000 (28), and evaluation of the reduced data quality by phenix.xtriage (29) revealed significant merohedral twinning no matter which space group was chosen, so the highest symmetry space group of $P2_13$ was selected for refinement (L test for acentric data value of 0.385, with perfect twin of 0.375 and twin law of l, −k, h). The structure of HypD was solved by molecular replacement using Phenix.phaser with the structure of dihydrodipicolinate synthase DapD from *Agrobacterium tumefaciens* (PDB code 2HMC), the sequence of which is 88% identical to that of HypD, as the search model for two copies in the asymmetric unit. B-factors were refined as isotropic using translation-libration-screw rotation (TLS) parameterization (groups were chain A residues 23 to 44, 45 to 129, 130 to 216, 217 to 280, and 281 to 340 and chain B residues 22 to 40, 41 to 45, 46 to 132, 133 to 213, and 214 to 340). The final atomic mode of HypD included residues 23 to 340 and 22 to 340 of the two chains in the asymmetric unit. The average B-factor and bond angle/length root mean square deviation (RMSD) values were calculated using Phenix. All model geometries were verified using the Phenix and Coot (30) validation tools plus the wwPDB validation server (31). The structure has good backbone with percentages of residues of 92.1% in the most favored, 7.5% in the additional allowed, 0% in the generously allowed, and 0.4% in the disallowed regions of the Ramachandran plot (corresponding to Leu-128 of each protein chain,

TABLE 1 Generation times of the Δ*hypO*, Δ*hypD*, Δ*hypH*, and Δ*hypS* mutants with various carbon sources

Strain	Result (h) with carbon source[a]:		
	L-Hyp	L-Proline	Sucrose
RmP110 (wild type)	5.3 (0.6)	6.0 (0.1)	4.2 (0.2)
RmP2514 (Δ*hypS*)	6.2 (0.6)	5.9 (0.2)	4.3 (0.1)
RmP2506 (Δ*hypO*)	10.2 (0.3)	6.0 (0.3)	4.4 (0.1)
RmP2510 (Δ*hypD*)	No growth	6.2 (0.3)	4.3 (0.2)
RmP2516 (Δ*hypH*)	10.2 (0.1)	6.1 (0.1)	4.2 (0.1)

[a] Values are the means from triplicate samples, with the standard deviations given in parentheses. Generation times were calculated between OD_{600} values of 0.1 and 0.3. L-Hyp, *trans*-4-hydroxy-L-proline.

TABLE 2 Kinetic parameters of the HypH α-ketoglutarate semialdehyde dehydrogenase enzyme

Parameter	Result for[a]:		
	α-KGSA	$NADP^+$	NAD^+
V_{max} (μmol^{-1} min^{-1} mg)	11	10	67
K_m (μM)[b]	40	47	1,420
k_{cat} (min^{-1})[c]	629	550	3,691
k_{cat}/K_m (μM^{-1} min^{-1})	16	12	0.06

[a] Values are the means from triplicate assays, and similar results were obtained in two independent experiments.
[b] The K_m for α-KGSA was determined with a constant concentration of 0.5 mM $NADP^+$. The K_m values for $NADP^+$ and NAD^+ were determined with a constant concentration of 178 μM α-KGSA.
[c] $k_{cat} = V_{max}[E]^{-1}$.

which is found at the noncrystallographic axis that is coincident with a putative protein-protein interface forming a HypD hexamer).

Structure similarity searches of the Protein Data Bank were performed using the PDBeFold and Dali servers (32, 33). Structure superpositions were performed with the Mustang algorithm (34). Protein-protein interfaces were determined using the PDBePISA server (35). Electrostatic potential surfaces were calculated using Chimera (36). The HypD active-site cavity was identified and analyzed using the CASTp server (37). PDB files were visualized with Jmol software (38).

The X-ray diffraction data collection statistics are listed in Table S1 in the supplemental material.

Protein structure accession number. The structure factors and atomic coordinates for the HypD complex structures were deposited in the Protein Data Bank with the PDB code 5CZJ.

RESULTS

Growth phenotypes of S. *meliloti hypD*, *hypH*, *hypO*, and *hypS* mutants. Previously in analyzing the *S. meliloti hyp* gene cluster, we showed that the *hypMNPQ* transport cassette and the *hypRE* epimerase gene are required for growth on hydroxyproline but that *hypY* (an epimerase-like pseudogene) is not (13, 14). To determine if the remaining predicted enzymes of the *hyp* gene cluster are required for growth on hydroxyproline, strains carrying nonpolar deletions of the *hypO*, *hypD*, *hypS*, and *hypH* genes were constructed, and the abilities of these strains to grow on various carbon sources were examined (Table 1). As all of the mutant strains grew at rates similar to that of the wild type in minimal medium with sucrose or L-proline as the carbon source, we conclude that the mutations appeared to have no effect on general carbon metabolism or L-proline catabolism (Table 1). With *trans*-4-L-Hyp as the sole source of carbon, the *hypD* mutant failed to grow, while the *hypO* and *hypH* mutants grew at about half the rate of the wild type, and, thus, these genes appear to play a role in *trans*-4-L-Hyp metabolism. The growth properties of the *hypS* mutant are discussed later.

***hypH* encodes an α-KGSADH.** To confirm that *hypH* encodes an α-ketoglutarate semialdehyde dehydrogenase (α-KGSADH) enzyme (EC 1.2.1.4), the *S. meliloti* HypH protein was purified from *E. coli* as an N-terminal His_6-tagged protein and assayed for α-KGSADH activity. As the α-ketoglutarate semialdehyde (α-KGSA) substrate used for assaying α-KGSADH is not commercially available, it was synthesized from D-glucarate using purified D-glucarate dehydratase and 5-keto-4-deoxy-glucarate dehydratase enzymes (see Materials and Methods and reference 25). The purified recombinant HypH protein catalyzed the NAD(P)-dependent reduction of α-KGSA, and the kinetic behavior of the enzyme at various concentrations of α-KGSA or $NADP^+$ or NAD^+ showed typical Michaelis-Menten hyperbolic kinetics (Table 2). The enzyme showed a clear preference for $NADP^+$ as a cofactor with a k_{cat}/K_m value for $NADP^+$ that was 200-fold higher than that for NAD^+ (Table 2). The substrate specificity of HypH was assessed using a standard reaction mix containing 0.5 mM $NADP^+$ and 1 mM aldehyde substrate. Specific activities of 21.1 ± 2.6, 0.8 ± 0.1, 1.1 ± 0.2, and 1.7 ± 0.2 μmol mg^{-1} min^{-1} were measured for α-KGSA, propionaldehyde (C_3), valeraldehyde (C_5), and octylaldehyde (C_8), respectively. This suggests that HypH activity is fairly specific for α-KGSA as a substrate.

The crystal structure of the *S. meliloti* HypH (Smb20262) protein was previously deposited in the Protein Data Bank (PDB code 3V4C); however, the specific role of the protein was not identified, and there is no associated publication. In addition, the amino acid sequence of HypH is 49% identical to that of an $NADP^+$-dependent aldehyde dehydrogenase (VH-ADH) from *Vibrio harveyi*, whose structural features involved in cofactor specificity and catalysis have been examined (PDB codes 1EZO and 1EYY) (39–42). Like HypH (Table 2), VH-ADH employs $NADP^+$ as a cofactor, and VH-ADH was shown to contain a cleft within which $NAD(P)^+$ binds. The adenine ring of $NADP^+$ interacts with the side chain and guanidium group of Arg-210 of VH-ADH (39), and in HypH, R-220 fulfills this role. In VH-ADH, there are extensive interactions between the 2′ phosphate of $NADP^+$ and Lys-172, Thr-175, and Arg-210, and the equivalent residues in HypH are Lys-182, Ser-185, and Arg-220. The small size of Thr-175 in VH-ADH provides a pocket in which the phosphate group from NADP can bind, and its small size is retained by Ser-185 of HypH. These structural data confirm the designation of HypH as an $NADP^+$-dependent α-KGSADH whose mechanism of cofactor specificity is conserved with that of VH-ADH.

***hypD* encodes an HPC deaminase.** The *S. meliloti hypD* gene is required for growth on *trans*-4-L-Hyp, and this phenotype was fully complemented by a plasmid carrying only the *hypD* gene (Table 1 and data not shown). We previously suggested that *hypD* encodes a Δ^1-pyrroline-4-hydroxy-2-carboxylate (HPC) deaminase that forms α-KGSA and NH_3 from HPC (14), and indeed, HypD shares 71% and 27% identity, respectively, with the HPC deaminase PP1257 protein from *P. putida* and the PA1254 protein from *P. aeruginosa* (12).

To verify that *hypD* encodes an HPC deaminase that converts HPC to α-KGSA and NH_3, the *S. meliloti* HypD protein was purified from *E. coli* as an N-terminal His_6-tagged protein and assayed for HPC deaminase activity. The HPC used in these assays

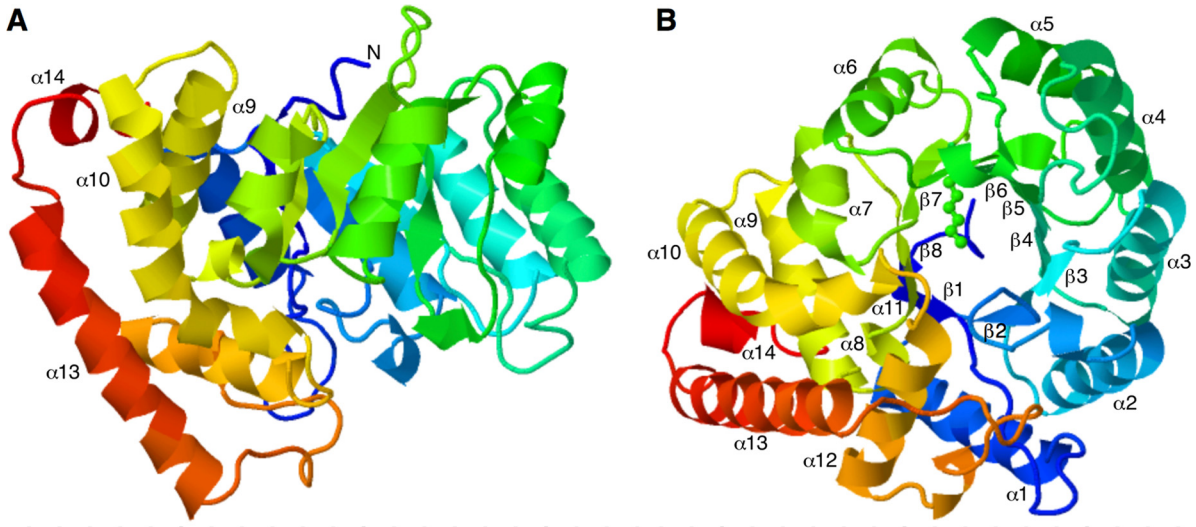

FIG 2 Schematic representation of the HypD crystal structure. (A) View from the "side" of the $(\alpha/\beta)_8$ barrel. The barrel motif is to the right of the image, and alpha helices 9, 10, 13, and 14 of the C-terminal extension are labeled (α9, α10, α13, and α14) for reference. The N terminus, starting at A3 in the refined structure, is labeled with an "N." (B) View "down" the barrel from the C-terminal face into the active site. The conserved active-site residue K184 is shown. All alpha helices are labeled (α1 to α14), as are the beta sheets (β1 to β8) of the $(\alpha/\beta)_8$ barrel motif. (A and B) Structures are colored from the N terminus (blue) to the C terminus (red).

was synthesized enzymatically from *cis*-4-D-Hyp, and the HPC deaminase activity was monitored by coupling its activity to α-KGSADH (see Materials and Methods). The purified HypD protein was found to catalyze the HPC-dependent formation of α-KGSADH with a specific activity of 1.6 μmol^{-1} min^{-1} mg^{-1} protein. The HypD-dependent formation of NH_3 from HPC was also detected via a glutamate dehydrogenase enzyme, but this assay was much less sensitive than the α-KGSADH-coupled assay. Because of the instability of the HPC substrate, further kinetic analysis of the HypD protein was not performed.

The HypD HPC deaminase protein is a member of the $(\alpha/\beta)_8$ barrel DapA family of proteins. Sequence analysis revealed that HypD is a member of the *N*-acetylneuraminate lyase (NAL) subfamily of $(\alpha/\beta)_8$ barrel proteins (EC 4.1.3.3). The enzymatic activities of a number of enzymes in this subfamily, including *Escherichia coli* dihydrodipicolinate synthase (DHDPS) (43), *E. coli* NAL (44), *Pseudomonas putida trans-o*-hydroxybenzylidenepyruvate hydratase-aldolase (HBPHA) (45), *P. putida* D-4-deoxy-5-oxoglucarate dehydratase (DOGDH) (46), and more recently *P. putida* Δ^1-pyrroline-4-hydroxy-2-carboxylate deaminase (LhpC), have been characterized (12). The HypD of *S. meliloti* characterized in this study has 31%, 26%, 26%, 27%, and 74% identities to the above-named enzymes, respectively (see Fig. S1 in the supplemental material). It is not surprising that HypD shows the highest identity to LhpC (74%) as they are homologous proteins that are involved in the same hydroxyproline catabolic pathway in *S. meliloti* and *P. putida* (12). The other proteins (DHDPS, NAL, HBPHA, and DOGDH) function in very different pathways: lysine biosynthesis, sialic acid concentration regulation, naphthalene degradation, and glucarate metabolism, respectively.

Although the DHDPS, NAL, HBPHA, and DOGDH enzymes function in disparate pathways, they all share a reaction mechanism with a covalent Schiff base intermediate that forms between the substrate (which varies, depending on the enzyme) and a completely conserved lysine residue in the active site (47). A tyrosine residue in the substrate binding pocket is also completely conserved and is predicted to be involved directly in the reaction mechanism or to function in stabilizing the position of the lysine (47, 48). The similarities of the sequences of HypD and LhpC to those of the other characterized members of this group and the fact that both have the conserved active-site lysine and tyrosine residues (see Fig. S1 in the supplemental material and reference 12) predict that the reaction mechanism of the bacterial HPC deaminase also involves a Schiff base intermediate.

The recombinant HypD protein was characterized in more detail through determination of the three-dimensional structure of the crystallized protein by X-ray crystallography. The asymmetric unit of the solved structure is two monomers, and putative protein-protein interfaces suggested the formation of a homotetramer. As predicted, each monomer has an $(\alpha/\beta)_8$ barrel fold with eight β sheets and eight α helices alternating from the N terminus toward the C terminus (Fig. 2). Consistently with other solved structures of the NAL subfamily, *E. coli* DHDPS and *E. coli* NAL (43, 44), HypD has a C-terminal extension beyond the last alpha helix (α8) of the barrel fold. The structures of HypD and *E. coli* DHDPS are very close; the deviation between the aligned alpha carbons of the two structures is 2.44 Å (see Fig. S2 in the supplemental material). The C-terminal extension of HypD consists of 6 alpha helices (α9 to α14). Together, α10 and α11 correspond to α10 of DHDPS, which has an extension of 5 alpha helices rather than 6.

In DHDPS and NAL, the active site is centered at the C-terminal face of the barrel (43, 44, 47). The lysine residue that is involved in Schiff base formation is extended in the substrate-binding pocket, with the conserved active-site tyrosine side chain just above it. In HypD, the positions of these residues, K164 and Y136, are extremely similar, with the lysine exposed for potential substrate binding (Fig. 2B). In the superposed structures of HypD and DHDPS, the deviation between K164 of HypD and the corresponding K161 of DHDPS (in both cases on β6) is 1.17Å (see Fig.

TABLE 3 Kinetic parameters of HypS in the reduction of Pyr2C and oxidation of L-proline

Parameter	Result for[a]:	
	Pyr2C	L-Proline
V_{max} (μmol^{-1} min^{-1} mg)	41	1.7
K_m (μM)	0.89	74
k_{cat} (min^{-1})[b]	1,469	61
k_{cat}/K_m (μM^{-1} min^{-1})	1,650	0.82

[a] Values are the means from triplicate assays, and similar results were obtained in two independent experiments. For the pyrroline-2-carboxylate (Pyr2C) reduction and L-proline oxidation reactions, NADPH and NADP$^+$ were present at concentrations of 0.5 mM and 1 mM, respectively.
[b] $k_{cat} = V_{max}\,[E]^{-1}$.

S2 in the supplemental material). These results strongly suggest that the reaction mechanism of HypD includes a covalent Schiff base intermediate which forms between the substrate and K164 in the enzyme's active site.

***hypS* encodes a P2C reductase that is required for growth with D-proline as the carbon source.** The HypS protein is annotated as a malate/L-lactate dehydrogenase family protein; however, assays with the purified His_6-tagged HypS protein showed no reduction in NAD(P)$^+$ with either malate or lactate as the substrate electron donor (data not shown). A screen for activity with other compounds identified L-proline as a substrate (Table 3). When Δ^1-pyrroline-2-carboxylate (P2C) was assayed as an electron acceptor, HypS was found to catalyze its NADPH-dependent reduction (Table 3). The pH optima for P2C reduction and L-proline oxidation were 10 and 7, respectively (data not shown). A kinetic analysis of P2C reduction and L-proline oxidation was performed (Table 3). The elevated k_{cat}/K_m with P2C as a substrate (2,914) compared to that of L-proline (0.87) showed that HypS has a clear preference toward the reduction of P2C to form L-proline (Table 3). This suggested that, under physiological conditions, HypS functions as a P2C reductase in the formation of L-proline.

Since the oxidation of D-proline produces Δ^1-pyrroline-2-carboxylate, we investigated whether wild-type *S. meliloti* and *hyp* mutants can grow on D-proline. The wild-type RmP110 and the *hypRE* and *hypD* mutants all grew on minimal medium containing 10 mM D-proline as the sole carbon source, whereas the *hypS* mutant failed to grow unless it was complemented in *trans* with an integrated copy of the *hypS* gene (Fig. 3B). Furthermore, the *hypO* and *hypMNPQ* mutants showed impaired growth with D-proline (see Fig. S3 in the supplemental material). The involvement of the *hyp* cluster in the catabolism of D-proline and the observed relatively slow growth of wild-type *S. meliloti* on D-proline (Fig. 3B) led us to investigate whether *hyp* gene transcription is induced by D-proline (Fig. 4). Reporter fusions of *gusA* to *hypM*, *hypS*, and the regulator *hypR* were found to be upregulated by D-proline relative to succinate or L-proline but to a lesser extent than L-Hyp (Fig. 4). As these results suggested that the slow growth of the wild type on D-proline may be caused by limited expression of some *hyp* genes, we tested a strain in which *hyp* transcription is constitutive because the negative regulator, *hypR*, was deleted. We found that the Δ*hypR* strain grew at a rate similar to that of the wild type on D-proline (data not shown), and hence *hyp* transcription does not appear to limit growth on D-proline.

Catabolism of D-proline proceeds via L-proline in *S. meliloti*. The finding that growth on D-proline required *hypS* suggested that

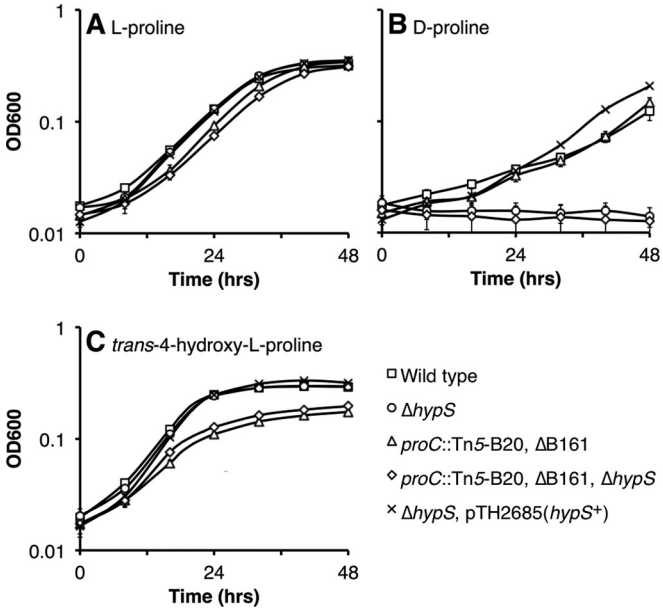

FIG 3 Growth profiles of *S. meliloti hypS* and related mutants. Shown are growth profiles of several *S. meliloti* strains in minimal medium containing as a sole source of carbon L-proline (A), D-proline (B), or *trans*-4-hydroxy-L-proline (C). Data points are the means from triplicate samples, and the error bars indicate the standard deviations. Strains shown are wild-type RmP110, RmP2514 (Δ*hypS*), RmP3155 (*proC*::Tn*5*-B20 ΔB161), RmP3153 (*proC*::Tn*5*-B20 ΔB161 Δ*hypS*), and RmP3272 [Δ*hypS* pTH2685(*hypS*$^+$)].

D-proline catabolism proceeds via Δ^1-pyrroline-2-carboxylate to L-proline, and a schematic diagram of this pathway is shown in Fig. 5. We performed two sets of experiments to confirm that D-proline is converted to L-proline in *S. meliloti*. First, we investigated whether mutants defective in L-proline utilization are also defective in the utilization of D-proline. In *S. meliloti*, L-proline is oxidized to glutamate by a proline dehydrogenase and a Δ^1-pyrroline-5-carboxylate dehydrogenase, with both enzyme activities present in the single bifunctional PutA protein (Fig. 5 and reference 49). We identified a *putA* mutant (SmFL5502) in our previously constructed pTH1522 reporter gene fusion library (21), and growth experiments employing this mutant revealed that the

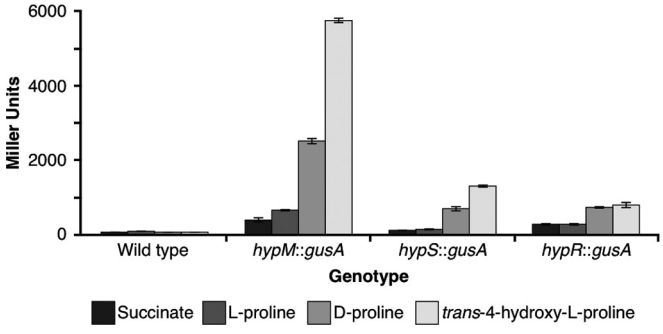

FIG 4 Induction profiles of the *hypM*, *hypS*, and *hypR* genes. The expression levels of the three *hyp* genes were measured following 40 h of growth in four different carbon sources using a *gusA* transcriptional fusion. β-Glucuronidase activities were derived from triplicate assays (±the standard errors of the mean), and similar results were obtained in two independent experiments. Strains shown are wild-type RmP110, RmP1886 (*hypM*::*gusA*), RmP239 (*hypS*::*gusA*), and RmFL2315 (*hypR*::*gusA*).

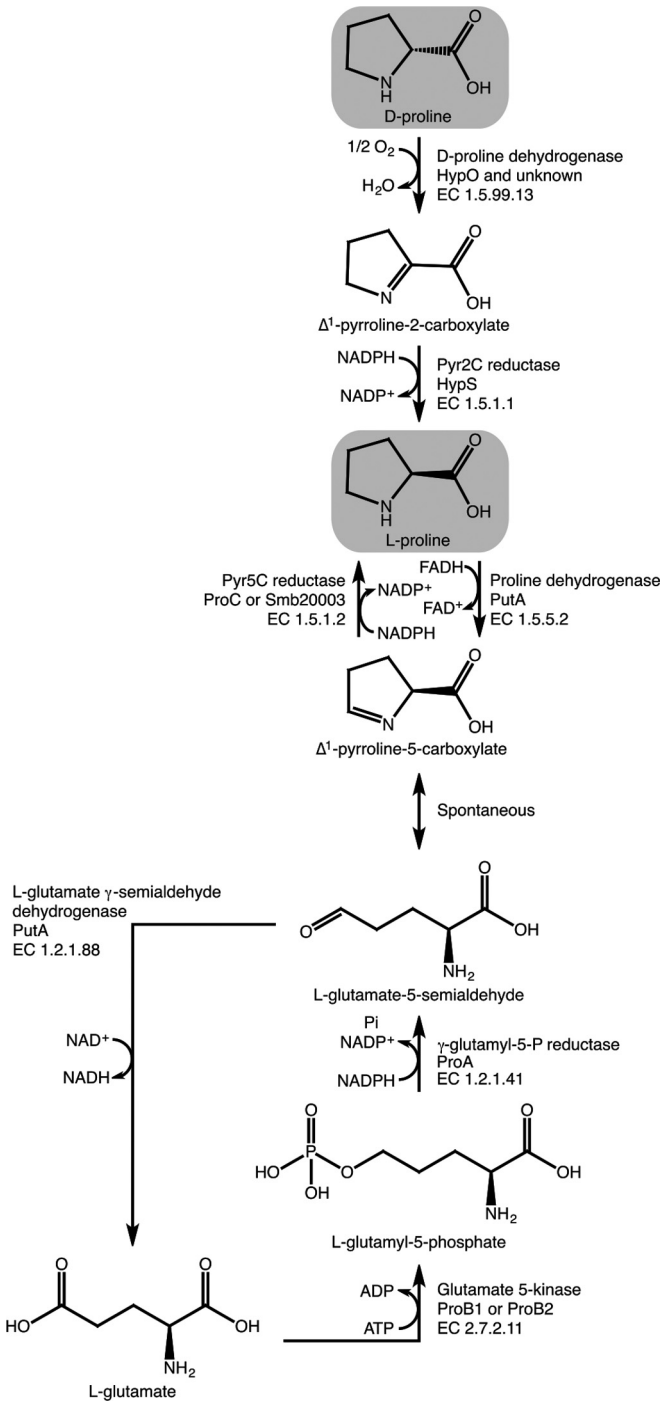

FIG 5 Schematic illustrations of L- and D-proline metabolism in *Sinorhizobium meliloti*. The biosynthetic and catabolic pathways for L-proline biosynthesis from L-glutamate are shown, as is the proposed pathway for D-proline catabolism. L-Proline and D-proline are highlighted by gray shading. The association of proteins to each biochemical reaction is based on the work reported here and elsewhere (20, 49, 64, 65, 67). Abbreviations: Pyr5C, Δ^1-pyrroline-5-carboxylate; Pyr2C, Δ^1-pyrroline-2-carboxylate; γ-glutamyl-5-P, γ-glutamyl-5-phosphate; Pi, phosphate.

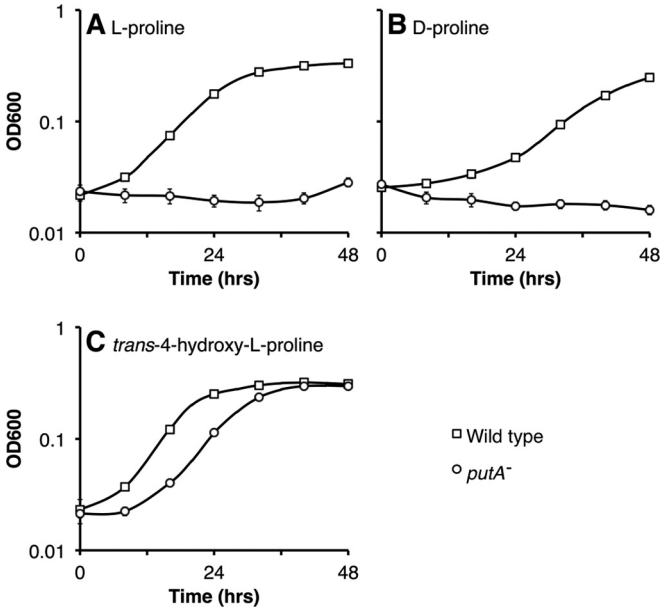

FIG 6 Effect of a *putA* mutation on growth with proline compounds. The growth profiles of wild-type *S. meliloti* RmP110 and *S. meliloti* RmFL5502 (*putA*::pTH1522) are shown in minimal medium containing as a sole source of carbon L-proline (A), D-proline (B), or *trans*-4-hydroxy-L-proline (C). Data points are the means from triplicate samples, and the error bars indicate the standard deviations.

growth of *S. meliloti* on L-proline or D-proline but not on *trans*-4-L-Hyp was dependent on *putA* (Fig. 6). A slight reduction in growth was observed for the *putA* mutant versus the wild type when grown with *trans*-4-L-Hyp as the carbon source, and we suggest that may result from constitutive expression of the reporter genes in the *putA*::*lacZ-gfp* fusion strain (21) (http://info.mcmaster.ca/fusionlibrary.html).

Catabolism of D-proline to L-proline predicts that growth of an *S. meliloti* L-proline auxotroph should occur whether the auxotroph is supplemented with L-proline or D-proline. To investigate this prediction, we employed an *S. meliloti* L-proline auxotroph with two genes disrupted, *proC* and *smb20003*, both of which encode Δ^1-pyrroline-5-carboxylate reductase enzymes required for L-proline synthesis (Fig. 5) (20). As this mutant (RmP3155) is unable to synthesize L-proline from L-glutamate, either L-proline supplementation or the addition of L-proline precursors for separate L-proline biosynthetic pathways is required for growth in minimal medium. When examined, this auxotroph grew in minimal medium containing either L-proline or D-proline (Fig. 3). We are aware of one other report in which an uncharacterized L-proline auxotroph of *P. putida* KT2440 grew upon supplementation of the medium with D-proline (50). Presumably, the growth resulting from that addition of D-proline would be dependent on the *dpkA*-encoded Δ^1-pyrroline-2-carboxylate reductase present in *P. putida* KT2440, although this was not tested (27).

DISCUSSION

We have presented evidence that *S. meliloti hypD* encodes an HPC deaminase and *hypH* an α-KGSADH, with each involved in the catabolism of *trans*-4-L-Hyp to α-KG (Fig. 1). As expected, *hypD* mutants failed to grow with *trans*-4-L-Hyp as the sole carbon source (Table 1). On the other hand, both *hypH* and *hypO* mutants continued to grow with *trans*-4-L-Hyp, albeit at half the rate of the wild type (Table 1). The partial-growth as opposed to the no-growth phenotype of the *hypH* and *hypO* mutants can be attributed to the presence of alternate enzyme activities. HypO is

predicted to be a *cis*-4-D-Hyp oxidase/dehydrogenase (14), and several proteins are annotated as D-amino acid oxidase enzymes in *S. meliloti*, e.g., Smb20877 and Smc03265. As these enzymes generally have broad specificity (51), it seems likely that the residual growth of the *hyp*O mutant on *trans*-4-L-Hyp is due to these oxidase activities; however, those enzymes were not examined further. A *cis*-4-D-Hyp dehydrogenase enzyme from *P. putida* was recently purified and characterized (12), and the sequence of that protein (PP1255) is 35% identical to that of the *S. meliloti* HypO protein. However, when *S. meliloti hypO* was cloned into expression plasmids, attempts to overexpress a His_6-tagged *S. meliloti* HypO protein either in *E. coli* or in *S. meliloti* were unsuccessful (data not shown). Thus, while we have not directly demonstrated an activity for HypO, its similarity to the *P. putida* PP1255 protein and the partial growth defect of the Δ*hypO* mutant with *trans*-4-L-Hyp as a carbon source support its role as a *cis*-4-D-Hyp dehydrogenase enzyme.

The *in vitro* catalysis of α-KGSA to α-KG by HypH (Table 2) showed that HypH can function as an α-KGSADH. α-KGSA dehydrogenase enzymes involved in the catabolism of L-arabinose, D-glucarate, D-galactarate, and hydroxy-L-proline have also been characterized (25, 52, 53). To investigate whether the reduced-growth phenotype of the *hypH* mutant on *trans*-4-L-Hyp may be due to the presence of other α-KGSADH-like enzymes, we searched the *S. meliloti* genome for other annotated dehydrogenases and identified the most similar as AraE, which functions as an α-KGSADH in the catabolism of L-arabinose (18). A *hypH araE* double mutant was constructed, and unlike the *hypH* mutant, which showed a moderate growth phenotype, and the *araE* mutant, which grew like the wild type, the *hypH araE* double mutant (RmP3174) failed to grow with *trans*-4-L-Hyp as the carbon source (data not shown). None of these strains had a growth defect with glucose as the sole carbon source. As the growth of the *hypH* mutant on *trans*-4-L-Hyp was dependent on *araE*, this growth presumably resulted from the activity of the *araE*-encoded α-KGSADH isoenzyme. This represents another example of genetic redundancy in *S. meliloti* (20), and taken together, these data illustrate that *hypH* encodes the primary α-KGSADH involved in the *trans*-4-L-Hyp catabolic pathway.

The inability of a *hypD*-null mutant to grow with *trans*-4-L-Hyp as a carbon source suggested that it is essential in the L-Hyp catabolic pathway. We previously suggested that *hypD* encodes a Δ^1-pyrroline-4-hydroxy-2-carboxylate (HPC) deaminase that forms α-KGSA and NH_3 from HPC (14). Additionally, LhpC (PP1257) of *P. putida*, which also catabolizes hydroxyproline, catalyzes the HPC deaminase reaction (12). In this study, we found that purified HypD is capable of converting HPC to α-KGSA and NH_3. Thus, HypD functions as the HPC deaminase in the L-Hyp catabolic pathway in *S. meliloti*.

HypD is a member of the *N*-acetylneuraminate lyase (NAL) subfamily of $(\alpha/\beta)_8$ barrel proteins, which includes the DHDPS, NAL, HBPHA, and DOGDH enzymes described above in Results. Consistent with what is known about the catalytic mechanism of these enzymes, the HypD structure has an $(\alpha/\beta)_8$ barrel fold with a C-terminal extension of alpha helices, and a putative active site which includes the conserved lysine and tyrosine residues (Fig. 2). The proposed mechanism for the NAL subfamily is the formation of a covalent Schiff base intermediate between the nitrogen of the active-site lysine side chain and substrate. However, the reactions catalyzed vary, depending on the enzyme, and include aldol cleavage, condensation, and decarboxylation (47, 48). Addition of HypD and LhpC to the subfamily adds deamination to the reactions performed by this group of proteins (12; this study).

Of the remaining uncharacterized genes in the *S. meliloti hyp* cluster, we have observed that *hypS* orthologs are often located in the vicinity of the *hypD* and *hypH* orthologs within genomes that carry *hyp* gene clusters (data not shown). However, a *hypS* mutant did not impact the ability of *S. meliloti* to grow with L-hydroxyproline. Characterization of HypS revealed that it functions as a Δ^1-pyrroline-2-carboxylate (P2C) reductase, forming L-proline, in an NADPH-dependent fashion (Table 3). HypS shares 41% amino acid identity with the NADPH-dependent P2C reductase DpkA protein from *P. putida* KT2440 (27), and the two showed similar kinetic properties because the reductase activities of both were inhibited by high concentrations of the substrate P2C (data not shown) and the two enzymes had similar pH optima. Although P2C is not an intermediate in the catabolism of *trans*-4-L-Hyp, it is in the catabolism of D-proline, and we showed that growth of *S. meliloti* on D-proline is dependent on HypS. HypMNPQ and HypO were also involved but were not essential for D-proline catabolism (see Fig. S3 in the supplemental material). These results are consistent with a metabolic pathway in *S. meliloti* through which D-proline is transported into the cell by the HypMNPQ uptake system, and it is subsequently oxidized to Δ^1-pyrroline-2-carboxylate by HypO and then converted to L-proline by HypS. A Δ*hypMNPQ* mutant was previously shown to grow poorly on *trans*-4-L-Hyp, and it was suggested that the residual growth likely resulted from *trans*-4-L-Hyp uptake via an alternate transport system (13). Similarly, HypMNPQ and HypO may transport and oxidize D-proline, and in their absence, other systems can partially fulfill these functions.

The above results prompted us to investigate whether the catabolic pathway for *trans*-4-L-Hyp might result in the synthesis of small quantities of D- or L-proline and hence whether the L-proline auxotroph might grow in minimal medium containing *trans*-4-L-Hyp (Fig. 3). Growth experiments revealed that incubation of a proline auxotroph (*proC smb20003*) with *trans*-4-L-Hyp (10 mM) resulted in slight growth; however, this growth was also observed for the *proC smb20003 hypS* triple mutant and hence was *hypS* independent (Fig. 3). We suspect that this is due to background ornithine cyclodeaminase activity, encoded by *ocd*, which can convert the L-arginine biosynthetic intermediate L-ornithine into L-proline (20, 54, 55), allowing partial growth of the *S. meliloti* L-proline auxotroph.

The ability of *S. meliloti* to metabolize and grow on D-proline coupled with the identified requirement for *hypS* in D-proline metabolism raises the question as to whether this is a primary role in the etiology of *hypS*. Low concentrations of D-proline have been detected in plants and soil, and hence the ability to catabolize D-proline might benefit the bacteria (56–58). However, an alternate role for *hypS* is in the reduction of Δ^1-pyrroline-2-carboxylate that is formed from the metabolism of *trans*-3-hydroxy-L-proline (*trans*-3-L-Hyp). Visser and coworkers identified a human *trans*-3-hydroxy-L-proline dehydratase enzyme, similar to proline racemases, which converts *trans*-3-L-Hyp to Δ^1-pyrroline-2-carboxylate (26). More recently, Watanabe and colleagues showed that *Azospirillum brasilense* can grow on *trans*-3-L-Hyp and that this ability is dependent on both a *trans*-3-L-Hyp dehydratase enzyme (GenBank accession no. AB894494.1) and a Δ^1-pyrroline-2-carboxylate reductase (GenBank accession no. AB845355.1), the

sequence of which is 51% identical to that of HypS (59). When tested, we found that *S. meliloti* cannot grow on *trans*-3-L-Hyp as a carbon source. Moreover, while the sequence of the *S. meliloti* HypY protein shows similarity to that of the *trans*-3-L-Hyp dehydratase (proline racemase), it lacks a cysteine residue important for catalysis and is presumably inactive for the dehydration reaction (14, 26, 59). We speculate that *hypS* is situated within the *hyp* cluster, as it was involved in the metabolism of hydroxyproline derivatives other than *trans*-4-L-Hyp, whose catabolism generates Δ^1-pyrroline-2-carboxylate.

The study of *hyp* genes in *S. meliloti* is also of interest because among the most highly expressed genes in N_2-fixing alfalfa bacteroids is a FixLJ microaerobically regulated gene, *smc03253* (60), which encodes a 2-oxoglutarate-dependent dioxygenase that converts L-proline to *cis*-4-hydroxy-L-proline (61). This raises the possibility that *cis*-4-Hyp could be synthesized by bacteroids (60), and if this occurred, we would expect to see induction of the *hyp* gene cluster during symbiosis (14). However, in alfalfa root nodules, the concentration of free hydroxyproline appears to be low, as the *S. meliloti hyp* genes are expressed at low levels in bacteroids (13).

In conclusion, the findings reported here and earlier (14) confirmed that *trans*-4-hydroxy-L-proline is catabolized to α-ketoglutarate in *S. meliloti* via the pathway shown in Fig. 1B. Together with other reports (12, 25, 59, 62–64), this report defines the genes that encode specific enzyme activities required for *trans*-4-hydroxy-L-proline catabolism. These studies should allow the identification of hydroxyproline catabolic genes in other organisms where many of these genes are annotated as genes of unknown function. In this respect, detailed knowledge of both the biochemistry and the regulation of the *hyp* genes of *S. meliloti* should be useful. The role of the *hyp* cluster in D-proline metabolism serves as a reminder that the *hyp* genes likely play roles in the metabolism of hydroxyproline- and proline-related compounds, many of which are found in plants, soils, and sediments (65, 66), as was recently shown for the osmolytes *trans*-4-hydroxy-L-proline betaine and *cis*-4-hydroxy-D-proline betaine (63).

ACKNOWLEDGMENTS

We thank Alain Perret for clones carrying the *A. baylyi* proteins ACIAD0128 and ACIAD0130 used for synthesis of α-KGSA, and Seiya Watanabe for clones carrying the *P. putida* and *P. aeruginosa cis*-4-hydroxy-D-proline dehydrogenase. We are grateful to Hannah MacKenzie, Guianeya Pérez Hernández, and James Boudreau for assistance in synthesis of α-ketoglutarate semialdehyde and HPC, and Philip Britz-McGibbon and the late Brian McCarry for interest and advice. We thank Aiping Dong at the Structural Genomics Consortium in Toronto, ON, Canada, for X-ray diffraction data collection.

FUNDING INFORMATION

Natural Science and Engineering Research Council of Canada provided funding to Turlough M. Finan.

This work was also supported by funding from the National Science and Engineering Research Council of Canada through an NSERC CGS-D scholarship to G.C.D. The funder had no role in study design, data collection and interpretation, or the decision to submit the work for publication.

REFERENCES

1. **Lawrence CC, Sobey WJ, Field RA, Baldwin JE, Schofield CJ.** 1996. Purification and initial characterization of proline 4-hydroxylase from *Streptomyces griseoviridis* P8648: a 2-oxoacid, ferrous-dependent dioxygenase involved in etamycin biosynthesis. Biochem J **313**(Part 1):185–191. http://dx.doi.org/10.1042/bj3130185.
2. **Shibasaki T, Mori H, Chiba S, Ozaki A.** 1999. Microbial proline 4-hydroxylase screening and gene cloning. Appl Environ Microbiol **65:**4028–4031.
3. **Gorres KL, Raines RT.** 2010. Prolyl 4-hydroxylase. Crit Rev Biochem Mol Biol **45:**106–124. http://dx.doi.org/10.3109/10409231003627991.
4. **Lamport DT, Miller DH.** 1971. Hydroxyproline arabinosides in the plant kingdom. Plant Physiol **48:**454–456. http://dx.doi.org/10.1104/pp.48.4.454.
5. **Kieliszewski MJ, O'Neill M, Leykam J, Orlando R.** 1995. Tandem mass spectrometry and structural elucidation of glycopeptides from a hydroxyproline-rich plant cell wall glycoprotein indicate that contiguous hydroxyproline residues are the major sites of hydroxyproline *O*-arabinosylation. J Biol Chem **270:**2541–2549. http://dx.doi.org/10.1074/jbc.270.6.2541.
6. **Wood KV, Stringham KJ, Smith DL, Volenec JJ, Hendershot KL, Jackson KA, Rich PJ, Yang WJ, Rhodes D.** 1991. Betaines of alfalfa: characterization by fast atom bombardment and desorption chemical ionization mass spectrometry. Plant Physiol **96:**892–897. http://dx.doi.org/10.1104/pp.96.3.892.
7. **Phillips DA, Sande ES, Vriezen JAC, de Bruijn FJ, Le Rudulier D, Joseph CM.** 1998. A new genetic locus in *Sinorhizobium meliloti* is involved in stachydrine utilization. Appl Environ Microbiol **64:**3954–2960.
8. **Burnet MW, Goldmann A, Message B, Drong R, Amrani El A, Loreau O, Slightom J, Tepfer D.** 2000. The stachydrine catabolism region in *Sinorhizobium meliloti* encodes a multi-enzyme complex similar to the xenobiotic degrading systems in other bacteria. Gene **244:**151–161. http://dx.doi.org/10.1016/S0378-1119(99)00554-5.
9. **Vranova V, Rejsek K, Skene KR, Formanek P.** 2011. Non-protein amino acids: plant, soil and ecosystem interactions. Plant Soil **342:**31–48. http://dx.doi.org/10.1007/s11104-010-0673-y.
10. **Moe LA.** 2013. Amino acids in the rhizosphere: from plants to microbes. Am J Bot **100:**1692–1705. http://dx.doi.org/10.3732/ajb.1300033.
11. **Adams E, Frank L.** 1980. Metabolism of proline and the hydroxyprolines. Annu Rev Biochem **49:**1005–1061. http://dx.doi.org/10.1146/annurev.bi.49.070180.005041.
12. **Watanabe S, Morimoto D, Fukumori F, Shinomiya H, Nishiwaki H, Kawano-Kawada M, Sasai Y, Tozawa Y, Watanabe Y.** 2012. Identification and characterization of D-hydroxyproline dehydrogenase and Δ^1-pyrroline-4-hydroxy-2-carboxylate deaminase involved in novel L-hydroxyproline metabolism of bacteria: metabolic convergent evolution. J Biol Chem **287:**32674–32688. http://dx.doi.org/10.1074/jbc.M112.374272.
13. **MacLean AM, White CE, Fowler JE, Finan TM.** 2009. Identification of a hydroxyproline transport system in the legume endosymbiont *Sinorhizobium meliloti*. Mol Plant Microbe Interact **22:**1116–1127. http://dx.doi.org/10.1094/MPMI-22-9-1116.
14. **White CE, Gavina JMA, Morton R, Britz-McKibbin P, Finan TM.** 2012. Control of hydroxyproline catabolism in *Sinorhizobium meliloti*. Mol Microbiol **85:**1133–1147. http://dx.doi.org/10.1111/j.1365-2958.2012.08164.x.
15. **Dobson RCJ, Valegård K, Gerrard JA.** 2004. The crystal structure of three site-directed mutants of *Escherichia coli* dihydrodipicolinate synthase: further evidence for a catalytic triad. J Mol Biol **338:**329–339. http://dx.doi.org/10.1016/j.jmb.2004.02.060.
16. **Yuan Z-C, Zaheer R, Finan TM.** 2006. Regulation and properties of PstSCAB, a high-affinity, high-velocity phosphate transport system of *Sinorhizobium meliloti*. J Bacteriol **188:**1089–1102. http://dx.doi.org/10.1128/JB.188.3.1089-1102.2006.
17. **Datsenko KA, Wanner BL.** 2000. One-step inactivation of chromosomal genes in *Escherichia coli* K-12 using PCR products. Proc Natl Acad Sci U S A **97:**6640–6645. http://dx.doi.org/10.1073/pnas.120163297.
18. **Poysti NJ, Loewen EDM, Wang Z, Oresnik IJ.** 2007. *Sinorhizobium meliloti* pSymB carries genes necessary for arabinose transport and catabolism. Microbiology **153:**727–736. http://dx.doi.org/10.1099/mic.0.29148-0.
19. **Milunovic B, diCenzo GC, Morton RA, Finan TM.** 2014. Cell growth inhibition upon deletion of four toxin-antitoxin loci from the megaplasmids of *Sinorhizobium meliloti*. J Bacteriol **196:**811–824. http://dx.doi.org/10.1128/JB.01104-13.
20. **diCenzo GC, Finan TM.** 2015. Genetic redundancy is prevalent within

the 6.7 Mb *Sinorhizobium meliloti* genome. Mol Genet Genomics **290:** 1345–1356. http://dx.doi.org/10.1007/s00438-015-0998-6.

21. **Cowie A, Cheng J, Sibley CD, Fong Y, Zaheer R, Patten CL, Morton RM, Golding GB, Finan TM.** 2006. An integrated approach to functional genomics: construction of a novel reporter gene fusion library for *Sinorhizobium meliloti*. Appl Environ Microbiol **72:**7156–7167. http://dx.doi.org/10.1128/AEM.01397-06.
22. **diCenzo GC, MacLean AM, Milunovic B, Golding GB, Finan TM.** 2014. Examination of prokaryotic multipartite genome evolution through experimental genome reduction. PLoS Genet **10:**e1004742. http://dx.doi.org/10.1371/journal.pgen.1004742.
23. **Singh RMM, Adams E.** 1965. Enzymatic deamination of Δ1-pyrroline-4-hydroxy-2-carboxylate to 2,5-dioxovalerate (α-ketoglutaric semialdehyde). J Biol Chem **240:**4344–4351.
24. **Yoneya T, Adams E.** 1961. Hydroxyproline metabolism. V. Inducible allohydroxy-D-proline oxidase of *Pseudomonas*. J Biol Chem **236:**3272–3279.
25. **Aghaie A, Lechaplais C, Sirven P, Tricot S, Besnard-Gonnet M, Muselet D, de Berardinis V, Kreimeyer A, Gyapay G, Salanoubat M, Perret A.** 2008. New insights into the alternative D-glucarate degradation pathway. J Biol Chem **283:**15638–15646. http://dx.doi.org/10.1074/jbc.M800487200.
26. **Visser WF, Verhoeven-Duif NM, de Koning TJ.** 2012. Identification of a human *trans*-3-hydroxy-L-proline dehydratase, the first characterized member of a novel family of proline racemase-like enzymes. J Biol Chem **287:**21654–21662. http://dx.doi.org/10.1074/jbc.M112.363218.
27. **Muramatsu H, Mihara H, Kakutani R, Yasuda M, Ueda M, Kurihara T, Esaki N.** 2005. The putative malate/lactate dehydrogenase from *Pseudomonas putida* is an NADPH-dependent Δ^1-piperideine-2-carboxylate/Δ^1-pyrroline-2-carboxylate reductase involved in the catabolism of D-lysine and D-proline. J Biol Chem **280:**5329–5335. http://dx.doi.org/10.1074/jbc.M411918200.
28. **Minor W, Cymborowski M, Otwinowski Z, Chruszcz M.** 2006. HKL-3000: the integration of data reduction and structure solution—from diffraction images to an initial model in minutes. Acta Crystallogr D Biol Crystallogr **62:**859–866. http://dx.doi.org/10.1107/S0907444906019949.
29. **Adams PD, Afonine PV, Bunkóczi G, Chen VB, Davis IW, Echols N, Headd JJ, Hung L-W, Kapral GJ, Grosse-Kunstleve RW, McCoy AJ, Moriarty NW, Oeffner R, Read RJ, Richardson DC, Richardson JS, Terwilliger TC, Zwart PH.** 2010. PHENIX: a comprehensive Python-based system for macromolecular structure solution. Acta Crystallogr D Biol Crystallogr **66:**213–221. http://dx.doi.org/10.1107/S0907444909052925.
30. **Emsley P, Cowtan K.** 2004. Coot: model-building tools for molecular graphics. Acta Crystallogr D Biol Crystallogr **60:**2126–2132. http://dx.doi.org/10.1107/S0907444904019158.
31. **Berman H, Henrick K, Nakamura H.** 2003. Announcing the worldwide Protein Data Bank. Nat Struct Biol **10:**980–980. http://dx.doi.org/10.1038/nsb1203-980.
32. **Holm L, Sander C.** 1994. Searching protein structure databases has come of age. Proteins **19:**165–173. http://dx.doi.org/10.1002/prot.340190302.
33. **Krissinel E, Henrick K.** 2004. Secondary-structure matching (SSM), a new tool for fast protein structure alignment in three dimensions. Acta Crystallogr D Biol Crystallogr **60:**2256–2268. http://dx.doi.org/10.1107/S0907444904026460.
34. **Konagurthu AS, Whisstock JC, Stuckey PJ, Lesk AM.** 2006. MUSTANG: a multiple structural alignment algorithm. Proteins **64:**559–574. http://dx.doi.org/10.1002/prot.20921.
35. **Krissinel E, Henrick K.** 2007. Inference of macromolecular assemblies from crystalline state. J Mol Biol **372:**774–797. http://dx.doi.org/10.1016/j.jmb.2007.05.022.
36. **Baker NA, Sept D, Joseph S, Holst MJ, McCammon JA.** 2001. Electrostatics of nanosystems: application to microtubules and the ribosome. Proc Natl Acad Sci U S A **98:**10037–10041. http://dx.doi.org/10.1073/pnas.181342398.
37. **Dundas J, Ouyang Z, Tseng J, Binkowski A, Turpaz Y, Liang J.** 2006. CASTp: computed atlas of surface topography of proteins with structural and topographical mapping of functionally annotated residues. Nucleic Acids Res **34:**W116–W118. http://dx.doi.org/10.1093/nar/gkl282.
38. **Hanson RM.** 2010. Jmol—a paradigm shift in crystallographic visualization. J Appl Crystallogr **43:**1250–1260. http://dx.doi.org/10.1107/S0021889810030256.
39. **Ahvazi B, Coulombe R, Delarge M, Vedadi M, Zhang L, Meighen E, Vrielink A.** 2000. Crystal structure of the $NADP^+$-dependent aldehyde dehydrogenase from *Vibrio harveyi*: structural implications for cofactor specificity and affinity. Biochem J **349**(Part 3):853–861. http://dx.doi.org/10.1042/bj3490853.
40. **Vedadi M, Meighen E.** 1997. Critical glutamic acid residues affecting the mechanism and nucleotide specificity of *Vibrio harveyi* aldehyde dehydrogenase. Eur J Biochem **246:**698–704. http://dx.doi.org/10.1111/j.1432-1033.1997.t01-1-00698.x.
41. **Vedadi M, Croteau N, Delarge M, Vrielink A, Meighen E.** 1997. Structural and functional studies of a $NADP^+$-specific aldehyde dehydrogenase from the luminescent marine bacterium *Vibrio harveyi*. Adv Exp Med Biol **414:**269–275.
42. **Vedadi M, Vrielink A, Meighen E.** 1997. Involvement of conserved glycine residues, 229 and 234, of *Vibrio harveyi* aldehyde dehydrogenase in activity and nucleotide binding. Biochem Biophys Res Commun **238:**448–451. http://dx.doi.org/10.1006/bbrc.1997.7300.
43. **Mirwaldt C, Korndörfer I, Huber R.** 1995. The crystal structure of dihydrodipicolinate synthase from *Escherichia coli* at 2.5 A resolution. J Mol Biol **246:**227–239. http://dx.doi.org/10.1006/jmbi.1994.0078.
44. **Izard T, Lawrence MC, Malby RL, Lilley GG, Colman PM.** 1994. The three-dimensional structure of *N*-acetylneuraminate lyase from *Escherichia coli*. Structure **2:**361–369. http://dx.doi.org/10.1016/S0969-2126(00)00038-1.
45. **Eaton RW.** 1994. Organization and evolution of naphthalene catabolic pathways: sequence of the DNA encoding 2-hydroxychromene-2-carboxylate isomerase and *trans-o*-hydroxybenzylidenepyruvate hydratase-aldolase from the NAH7 plasmid. J Bacteriol **176:**7757–7762.
46. **Jeffcoat R, Hassall H, Dagley S.** 1969. Purification and properties of D-4-deoxy-5-oxoglucarate hydro-lyase (decarboxylating). Biochem J **115:**977–983. http://dx.doi.org/10.1042/bj1150977.
47. **Lawrence MC, Barbosa JA, Smith BJ, Hall NE, Pilling PA, Ooi HC, Marcuccio SM.** 1997. Structure and mechanism of a sub-family of enzymes related to *N*-acetylneuraminate lyase. J Mol Biol **266:**381–399. http://dx.doi.org/10.1006/jmbi.1996.0769.
48. **Barbosa JA, Smith BJ, DeGori R, Ooi HC, Marcuccio SM, Campi EM, Jackson WR, Brossmer R, Sommer M, Lawrence MC.** 2000. Active site modulation in the *N*-acetylneuraminate lyase sub-family as revealed by the structure of the inhibitor-complexed *Haemophilus influenzae* enzyme. J Mol Biol **303:**405–421. http://dx.doi.org/10.1006/jmbi.2000.4138.
49. **Jiménez-Zurdo JI, García-Rodríguez FM, Toro N.** 1997. The *Rhizobium meliloti putA* gene: its role in the establishment of the symbiotic interaction with alfalfa. Mol Microbiol **23:**85–93. http://dx.doi.org/10.1046/j.1365-2958.1997.1861555.x.
50. **Molina-Henares MA, la Torre de, García-Salamanca JA, Molina-Henares AJ, Herrera MC, Ramos JL, Duque E.** 2010. Identification of conditionally essential genes for growth of *Pseudomonas putida* KT2440 on minimal medium through the screening of a genome-wide mutant library. Environ Microbiol **12:**1468–1485.
51. **Pollegioni L, Motta P, Molla G.** 2013. L-Amino acid oxidase as biocatalyst: a dream too far? Appl Microbiol Biotechnol **97:**9323–9341. http://dx.doi.org/10.1007/s00253-013-5230-1.
52. **Brouns SJJ, Walther J, Snijders APL, van de Werken HJG, Willemen HLDM, Worm P, de Vos MGJ, Andersson A, Lundgren M, Mazon HFM, van den Heuvel RHH, Nilsson P, Salmon L, de Vos WM, Wright PC, Bernander R, van der Oost J.** 2006. Identification of the missing links in prokaryotic pentose oxidation pathways: evidence for enzyme recruitment. J Biol Chem **281:**27378–27388. http://dx.doi.org/10.1074/jbc.M605549200.
53. **Watanabe S, Yamada M, Ohtsu I, Makino K.** 2007. alpha-Ketoglutaric semialdehyde dehydrogenase isozymes involved in metabolic pathways of D-glucarate, D-galactarate, and hydroxy-L-proline. Molecular and metabolic convergent evolution. J Biol Chem **282:**6685–6695.
54. **Soto MJ, van Dillewijn P, Olivares J, Toro N.** 1994. Ornithine cyclodeaminase activity in *Rhizobium meliloti*. FEMS Microbiol Lett **119:**209–213. http://dx.doi.org/10.1111/j.1574-6968.1994.tb06890.x.
55. **diCenzo GC, Zamani M, Cowie A, Finan TM.** 2015. Proline auxotrophy in *Sinorhizobium meliloti* results in a plant-specific symbiotic phenotype. Microbiology **161:**2341–2351. http://dx.doi.org/10.1099/mic.0.000182.
56. **Kimber RWL, Nannipieri P, Ceccanti B.** 1990. The degree of racemization of amino acids released by hydrolysis of humic-protein complexes: implications for age assessment. Soil Biol Biochem **22:**181–185. http://dx.doi.org/10.1016/0038-0717(90)90084-D.

57. **Brückner H, Westhauser T.** 2003. Chromatographic determination of L- and D-amino acids in plants. Amino Acids **24:**43–55.
58. **Brodowski S, Amelung W, Lobe I, Du Preez CC.** 2004. Losses and biogeochemical cycling of soil organic nitrogen with prolonged arable cropping in the South African Highveld—evidence from L- and D-amino acids. Biogeochemistry **71:**17–42. http://dx.doi.org/10.1007/s10533-004-5733-z.
59. **Watanabe S, Tanimoto Y, Yamauchi S, Tozawa Y, Sawayama S, Watanabe Y.** 2014. Identification and characterization of *trans*-3-hydroxy-L-proline dehydratase and Δ^1-pyrroline-2-carboxylate reductase involved in *trans*-3-hydroxy-L-proline metabolism of bacteria. FEBS Open Bio **4:**240–250. http://dx.doi.org/10.1016/j.fob.2014.02.010.
60. **Ferrières L, Francez-Charlot A, Gouzy J, Rouillé S, Kahn D.** 2004. FixJ-regulated genes evolved through promoter duplication in *Sinorhizobium meliloti*. Microbiology **150:**2335–2345. http://dx.doi.org/10.1099/mic.0.27081-0.
61. **Hara R, Kino K.** 2009. Characterization of novel 2-oxoglutarate dependent dioxygenases converting L-proline to *cis*-4-hydroxy-L-proline. Biochem Biophys Res Commun **379:**882–886. http://dx.doi.org/10.1016/j.bbrc.2008.12.158.
62. **Zhao S, Sakai A, Zhang X, Vetting MW, Kumar R, Hillerich B, San Francisco B, Solbiati J, Steves A, Brown S, Akiva E, Barber A, Seidel RD, Babbitt PC, Almo SC, Gerlt JA, Jacobson MP.** 2014. Prediction and characterization of enzymatic activities guided by sequence similarity and genome neighborhood networks. Elife **3:**1005.
63. **Zhao S, Kumar R, Sakai A, Vetting MW, Wood BM, Brown S, Bonanno JB, Hillerich BS, Seidel RD, Babbitt PC, Almo SC, Sweedler JV, Gerlt JA, Cronan JE, Jacobson MP.** 2013. Discovery of new enzymes and metabolic pathways by using structure and genome context. Nature **502:**698–702. http://dx.doi.org/10.1038/nature12576.
64. **Watanabe S, Tanimoto Y, Nishiwaki H, Watanabe Y.** 2015. Identification and characterization of bifunctional proline racemase/hydroxyproline epimerase from archaea: discrimination of substrates and molecular evolution. PLoS One **10:**e0120349. http://dx.doi.org/10.1371/journal.pone.0120349.
65. **Dunn MF.** 2015. Key roles of microsymbiont amino acid metabolism in rhizobia-legume interactions. Crit Rev Microbiol **41:**411–451. http://dx.doi.org/10.3109/1040841X.2013.856854.
66. **Servillo L, Giovane A, Balestrieri ML, Cautela D, Castaldo D.** 2011. Proline derivatives in fruits of bergamot (*Citrus bergamia* Risso et Poit): presence of N-methyl-L-proline and 4-hydroxy-L-prolinebetaine. J Agric Food Chem **59:**274–281. http://dx.doi.org/10.1021/jf102833v.
67. **Jiménez-Zurdo JI, van Dillewijn P, Soto MJ, de Felipe MR, Olivares J, Toro N.** 1995. Characterization of a *Rhizobium meliloti* proline dehydrogenase mutant altered in nodulation efficiency and competitiveness on alfalfa roots. Mol Plant Microbe Interact **8:**492–498. http://dx.doi.org/10.1094/MPMI-8-0492.